




Observation of the algebraic localization-delocalization transition in a one-dimensional disordered potential with a bias force

G. Berthet, L. Lavoine, M. K. Parit , A. Brolis , A. Boissé, and T. Bourdel 

Laboratoire Charles Fabry, Institut d'Optique Graduate School, CNRS, Université Paris-Saclay, 2 avenue A. Fresnel, 91127 Palaiseau Cedex, France



(Received 2 August 2019; accepted 30 January 2020; published 31 March 2020)

One-dimensional (1D) Anderson localization phenomena are strongly affected by a bias force or equivalently a voltage in electronic systems. We experimentally study this case, launching a noninteracting ^{39}K Bose-Einstein condensate in a 1D disordered potential induced by a far-off-resonance laser speckle, while controlling a bias force. In agreement with theoretical predictions, we observe a transition between algebraic localization and delocalization as a function of our control parameter that is the relative strength of the disorder against the bias force. We also demonstrate that the transition is intrinsically energy independent and that the initial velocity of the wave packet only plays a role through an effective disorder strength due to the correlation of the disorder.

DOI: [10.1103/PhysRevResearch.2.013386](https://doi.org/10.1103/PhysRevResearch.2.013386)

I. INTRODUCTION

Adding a bias force is a quite natural way to probe the transport properties of quantum systems, a subject of broad interest. In particular, electronic systems are probed through the current response to an applied voltage that is equivalent to a force. The study of transport with atomic quantum gases is of specific interest because of their high degree of control and versatility. They do not suffer from dissipation or decoherence effects, such as the ones induced by phonons in condensed-matter materials [1]. For example, Bloch oscillations have been measured through the addition of a constant force to atoms in a periodic potential induced by an optical lattice [2]. A force applied to a harmonic trap is equivalent to a trap displacement. The response to such a displacement reveals the fluid or insulating behavior of atomic systems. In one-dimensional (1D) interacting Bose gases, the pinning transition by an optical lattice [3,4] or the insulating transition in quasidisordered optical lattice [5,6] have been studied in this manner. More recently, transport in quantum gases is also studied in biased junction-type setup more analogous to condensed-matter systems [7,8].

In our work, we focus on the transport of noninteracting particles in disordered media. Without a bias force, quantum interferences between multiple paths lead to Anderson localization [9] whose signature is an exponential decay in the space of single-particle wave functions [10]. This phenomenon is ubiquitous in wave and quantum physics and it has been observed in many physical contexts [11] including condensed matter [12] and ultracold atoms [13–15]. One-dimensional truly disordered systems are always localized

[16], unlike the three-dimensional (3D) cases where a localization transition takes place [17–20].

The localization properties of 1D disordered systems are strongly modified in the presence of a bias force. At infinite time, theoretical studies predict a sharp localization-delocalization transition as a function of a single dimensionless parameter α which is the ratio of the force to the disorder strength [21,22]. The transition remarkably does not depend on the energy of the particles for a white noise disorder. In addition, the usual exponential decay associated to the localization is replaced by a much weaker algebraic decay. Related phenomena such as a nonlinear current-voltage response could be relevant in 1D condensed-matter systems such as nanowires [23] or nanotubes [12].

Realistic disorders can be correlated with possible important effects. For particles at momentum k , only disorder Fourier components around $2k$ are relevant in the weak disorder limit (Born approximation). For example, our disorder produced from a far-off-resonance laser speckle [24] has no Fourier component beyond a spatial frequency k_c and backscattering and localization are thus not expected for atoms with wave vectors $k > k_c/2$ (effective mobility edge) [13,25]. Since localized wave functions always have a small fraction at long distances corresponding to large energies and momenta, in the presence of a bias force, we thus expect correlation-induced delocalization at very long times. However, at transient times, sufficiently fine disorder correlations are expected to play little role [22].

In this paper, we report on the observation of the algebraic localization-delocalization transition with ultracold atoms propagating in a one-dimensional disordered potential in the presence of a controlled bias force. We experimentally show that the dimensionless ratio of the force to the disorder strength α is the only relevant parameter to describe the transition. We notice that the initial velocity of the quantum wave packet only plays a role through the correlation of the disordered potential, showing that the transition is intrinsically energy independent. In the localized regime, we

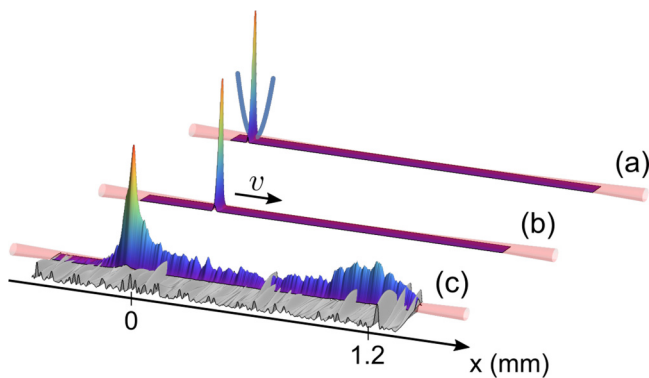


FIG. 1. Schematic of the experimental sequence. A noninteracting atomic Bose-Einstein condensate is produced in a crossed trap (a). The cloud is then launched into a 1D tube with a controlled force (b). The cloud can be accelerated to a velocity v . A constant force is then applied for a time τ to the system while a 1D speckle at 532 nm is shone on the atoms (c). An average density profile over eight disorder realizations is shown.

demonstrate an algebraic decay of the density and measure the corresponding decay exponent as a function of α , revealing features due to the speckle disorder correlation.

II. EXPERIMENTAL SETUP

We first produce a ^{39}K Bose-Einstein condensate. In contrast to our previous works [26–28], after optical cooling, we pump the atoms to the $|F = 2, m_F = 2\rangle$ state and load a magnetic trap which serves as a reservoir for loading a tightly confining optical trap [29]. The evaporation is then pursued in the $|F = 1, m_F = 1\rangle$ state in the vicinity of the 403.4(7) G Feshbach resonance [30] until condensation is reached. The magnetic field is then ramped down close to the scattering length zero crossing at 350.4(4) G in order to be in a noninteracting regime. The scattering length is then $-0.2 \pm 0.2 a_0$ with a_0 being the Bohr radius. The final trap is made of two horizontal far-detuned laser beams at 1064 and 1550 nm. Its trapping frequencies are $18 \times 124 \times 124$ Hz. When the 1550-nm beam is turned off, the longitudinal confinement (along \hat{x}) is removed and the atoms are free to evolve in the 1064-nm trap whose radial frequencies are $\omega_{\perp}/2\pi = 124$ Hz [31] (see Fig. 1). The residual trapping frequency in the longitudinal direction is precisely canceled to 0.0(5) Hz by using the magnetic field curvature induced by two pairs of magnetic coils. We also control a longitudinal force, characterized by an acceleration a , through a magnetic field gradient produced by an off-centered additional coil.

A 1D disorder potential is shone on the atoms for a time τ while they propagate in the one-dimensional trap under the action of the constant force. The atoms are finally imaged by resonant fluorescence imaging at zero magnetic field. For a strong disorder, the atoms do not move much from their initial position, whereas, for small disorder, they behave ballistically. We adjust the propagation time τ as a function of the constant force such that in the ballistic regime the atoms travel about 1 mm and are still in the camera field of view. In this case, the velocity spread of the atomic cloud is measured to be $\Delta v = 0.37(6) \text{ mm s}^{-1}$. In Fig. 1(c), we show

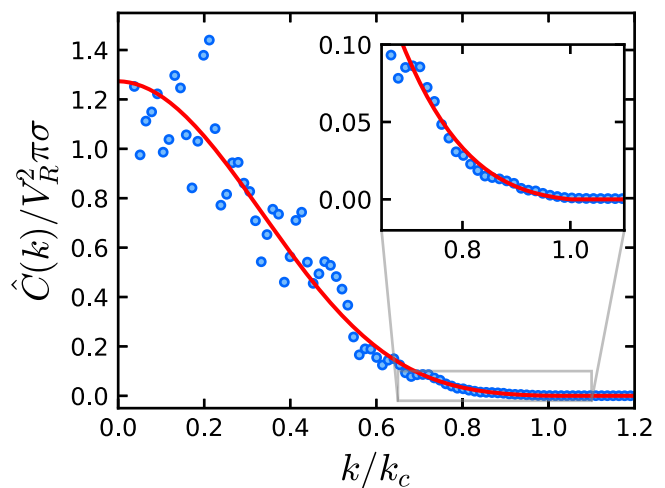


FIG. 2. Power spectral function $\hat{C}(k)$ of a single realization of the disorder measured in a square of $175 \times 175 \mu\text{m}$. The dispersal of points at low spatial frequencies is due to the speckle randomness. The curve is a fit with the autoconvolution of a truncated Gaussian as can be experimentally expected from a truncated Gaussian entering the optical system. The fitted function is used in the rest of the paper. The inset shows an enlargement around $k/k_c = 1$.

a density profile observed at intermediate disorder strength where both localized and ballistic atomic fraction are visible. We define the localized fraction by integrating over a window extending by $300 \mu\text{m}$ in the propagation direction. This value is chosen somewhat arbitrarily to include most atoms in the localized decaying peak while not including atoms that are in the process of escaping. We have checked that our experimental results do not strongly depend on the chosen value [32].

The disorder is produced from a laser speckle at 532 nm, and its effect on the atoms is the one of a conservative potential. The 532-nm laser beam propagates along the \hat{z} axis and passes through a diffusing plate. The amplitude V_R of the speckle potential is proportional to the laser intensity and corresponds to both its mean value and its standard deviation [24]. On the diffusing plate, the intensity distribution is elliptical with the major axis along \hat{x} and the minor axis along \hat{y} . This produces an anisotropic disorder that we have imaged for characterization. The autocorrelation widths are $4.7 \mu\text{m}$ along \hat{y} and $4.3 \mu\text{m}$ along \hat{z} (half-width at $1/\sqrt{e}$). Both values largely exceeds the ground-state extension of the harmonic oscillator $\sqrt{\hbar/2m\omega_{\perp}} = 1.0 \mu\text{m}$, where m is the atomic mass and \hbar is the reduced Planck constant. The disordered potential can thus be considered as one dimensional for the atoms propagating along \hat{x} . In this direction, the power spectral density $\hat{C}(k)$ is shown in Fig. 2. It takes zero values for wave vectors larger than $k_c = 2/\sigma$ with $\sigma = 0.34(1) \mu\text{m}$. The power spectral density at zero momentum is $\hat{C}(k=0) = cV_R^2\pi\sigma$, where $c = 1.26(5)$. It would be 1 for a uniform intensity on the diffusing plate.

Let us now discuss the relevant energy scales of our experiment. The correlation length of the disorder gives the correlation energy $E_{\sigma} = \hbar^2/2m\sigma^2 = (2\pi\hbar) \times 1.1 \text{ kHz}$. In order for the correlation of the disorder to play little role, it has to be the largest energy scale. By dimensional analysis,

one can construct an energy scale $E_a = \hbar^{2/3} m^{1/3} a^{2/3}$ associated with the acceleration a . Experimentally, E_a takes values between $(2\pi\hbar) \times 7$ Hz and $(2\pi\hbar) \times 33$ Hz. The disorder strength is characterized by V_R , which is varied between 0 and $(2\pi\hbar) \times 200$ Hz. A more relevant parameter when comparing with a white noise potential is rather $V^* = \hbar^{-2/3} m^{1/3} \hat{C}(0)^{2/3}$, which is lower than V_R . The dimensionless parameter α is then defined as $\alpha = (E_a/V^*)^{3/2} = \hbar^2 a / \hat{C}(0)$ such that the localization-delocalization transition is expected for $\alpha = 1$ [22]. Another energy scale, $E_\tau = \hbar/\tau$, can be associated to the propagation time τ . Its value is chosen to be below the value of E_a by a factor of the order of 15 to 20, such that propagation, scattering, and localization phenomena have enough time to set in. Note that in a correlated speckle disorder, the very long time limit is complete delocalization [22] and we thus work at intermediate time where the localization-delocalization transition is smoothed.

III. RESULTS

We first study the case of atoms entering the disorder without initial velocity. The localized fraction are measured for four different values of the acceleration $a = 9.3(6)$, $a = 19(1)$, $a = 32(2)$, and $a = 81(4)$ mm s⁻² respectively associated with propagation times $\tau = 460$, $\tau = 320$, $\tau = 280$, $\tau = 90$ ms [see Fig. 3(a)]. For small values of the speckle amplitude V_R , the system is mostly delocalized whatever the acceleration. On the contrary, all the atoms are localized when the speckle strength is high. One notes slower acceleration is correlated with faster localized fraction increases with V_R .

Rescaling the horizontal axis with the dimensionless parameter $1/\sqrt{\alpha}$, which is proportional to V_R/\sqrt{a} , leads to a clear collapse of the data within the error bars [see Fig. 3(b)]. This indicates that α , which compares the acceleration to the disorder strength, is the relevant parameter driving the localization-delocalization transition. If the transition point is defined for a localized fraction equal to 0.5, this corresponds to $\alpha = 1.0(3)$. We can compare these results with disorder-averaged numerical simulations of the 1D Schrödinger equation for our parameters [Fig. 3(b)]. We use these simulations to calibrate V_R as a function of the optical power with a 15% uncertainty, matching estimations from scattering experiments in the absence of a force.

We now consider the case of atoms entering the disorder with an initial positive velocity. The initial velocity v is first set by applying an acceleration to the atoms during 10 ms without disorder (see Fig. 1). The acceleration is then changed to its final value $a = 19$ mm s⁻² and the speckle is shone on the atoms for 280 ms. The measured localized fractions are presented in Fig. 4 [28]. For the highest velocity ($v = \hbar k/m = 2.9$ mm s⁻¹), $k\sigma_x \simeq 0.6$, and the value of the disorder potential's power spectrum $\hat{C}(2k) = 0.17\hat{C}(0)$ is greatly reduced. This correlation effect is responsible for the noncollapsing behavior when the localized fractions are plotted as a function of $1/\sqrt{\alpha}$ [see Fig. 4(a)]. Plotting as a function of $1/\sqrt{\alpha^*}$, where $\alpha^* = \hbar^2 a / \hat{C}(2k)$ takes into account an effective disorder strength at the atomic initial momentum k , leads to a much better collapse of the data on the curve at zero velocity for which $\alpha^* = \alpha$ [see Fig. 4(b)]. This indicates that α^* is

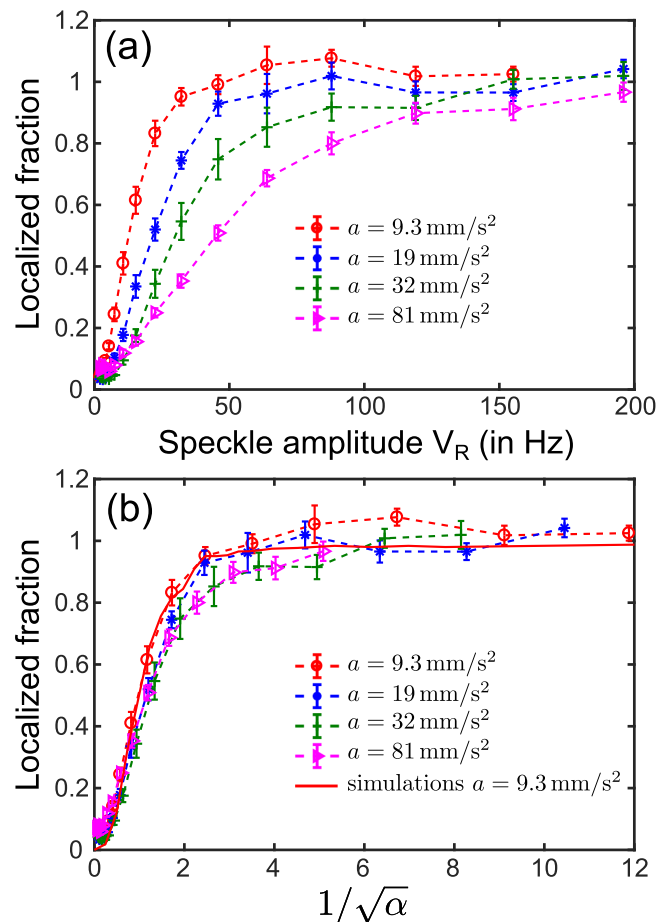


FIG. 3. Localized atomic fraction as a function of the speckle amplitude V_R (a) and $1/\sqrt{\alpha} \propto V_R/\sqrt{a}$ (b) obtained for four different values of the applied acceleration and $v = 0$. Each curve is averaged over eight realizations of the disorder potential. The error bars are the standard deviations of the measured localized fractions. Experimental values above 1 are due to small errors in background subtraction. The continuous red line is the average of numerical simulations of the 1D Schrödinger equation.

the most relevant parameter and that the initial velocity only plays a role through the correlation of the disorder [22]. The transition point corresponding to a localized fraction of 0.5 is obtained for $\alpha^* = 1.0(4)$ [Fig. 4(b)].

Finally, we perform a more careful analysis of the localized profiles for the specific case of $a = 19$ mm s⁻². We find that single profiles are quite noisy with modulations that are stable for a given speckle realization. This shows that the localization profile is not a self-averaging quantity. We thus average results for eight different realizations of the speckle in order to obtain smooth localization profiles (Fig. 5). An algebraic scaling is visible for distances between 40 and 300 μ m (a straight line in log-log scale), whereas an exponential decay in this region does not fit the data. It is expected that the algebraic dependence is only valid at sufficiently large distances [22,33]. Above 300 μ m, the signal-to-noise ratio is low.

We now study the algebraic decay coefficient β as a function of the disorder strength or equivalently as a function of α^* (see Fig. 6). The coefficient is found to increase

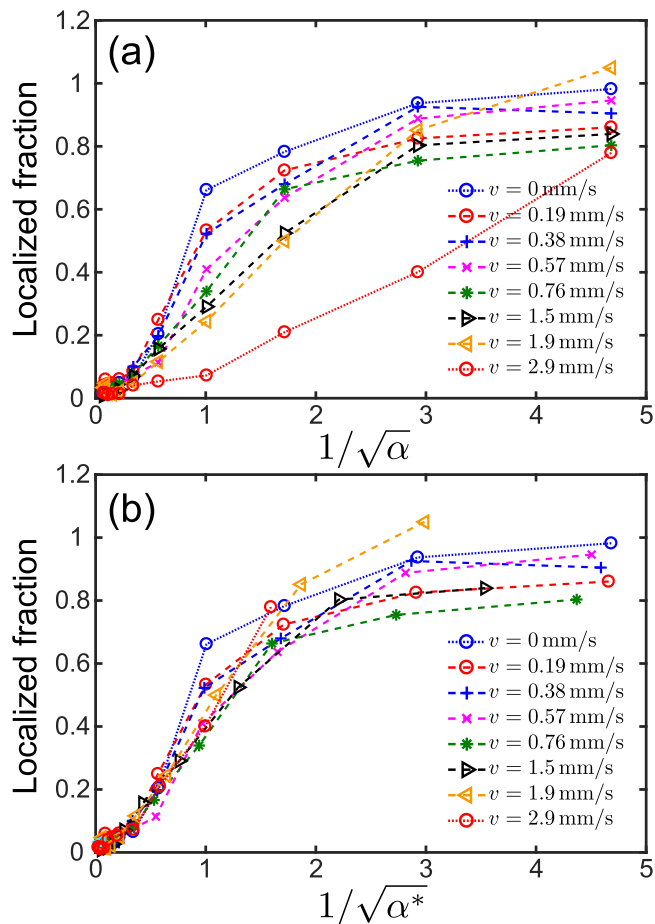


FIG. 4. Localized fractions of the noninteracting cloud of atoms as a function of $1/\sqrt{\alpha}$ (a) and $1/\sqrt{\alpha^*}$ (b) for different values of the initial velocity and $a = 19 \text{ mm s}^{-2}$.

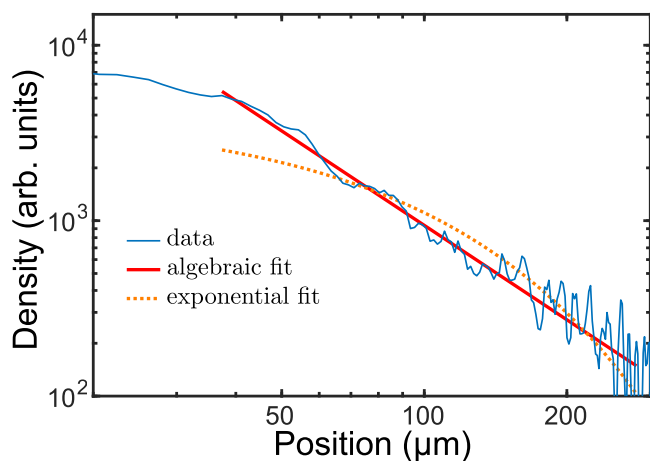


FIG. 5. Averaged localized density profile as a function of the atom displacement in log-log scale for $a = 19 \text{ mm s}^{-2}$, $\alpha = 0.03$, and $v = 0$. Log-log scale permits us to show the algebraic dependence as a straight line. The algebraic (red continuous line) and exponential (orange dotted line) fits are displayed. The fit with the power law $1/x^\beta$ leads to $\beta = 1.79 \pm 0.10$, where the error bar is evaluated from reduced data sets of four speckle realizations.

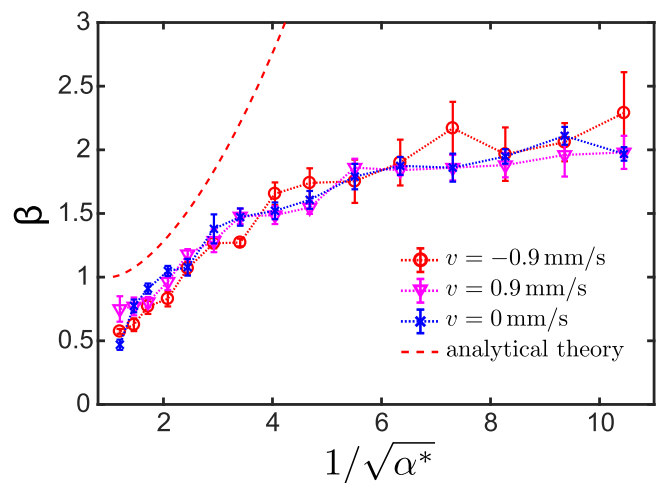


FIG. 6. Values of β , obtained by fitting to the localized density profile with a power law, as a function of $1/\sqrt{\alpha^*}$ for three different values of the initial velocity and $a = 19 \text{ mm s}^{-2}$.

with increasing disorder as can be expected for stronger localization effects. Moreover, we show that the behavior is not modified by a small positive or negative initial velocity ($v = \pm 0.9 \text{ mm s}^{-1}$) as expected theoretically. However, our results do not match with the infinite time white-noise analytical exponents from Ref. [22] (dashed line in Fig. 6). For small disorder, the small mismatch can be due to the fact that the measurement of β is sensitive to the wings of the density distribution up to distances of $300 \mu\text{m}$, where the atom momentum k has significantly increase and $\hat{C}(2k)$ cannot be considered constant at this scale. The observed saturation of β at large disorder is a striking deviation that we interpret as a consequence of a strong and correlated disorder. A strong disorder ($V_R \sim E_\sigma$) broadens the initial wave-vector distribution such that k vectors around $1/\sigma$ are populated as can be understood from the broad width of the spectral functions [34,35]. In this case, even in the absence of a force, the diverging behavior of the localization length close to the effective mobility edge $1/\sigma$ is responsible for an algebraic decay of the localized density profiles with a coefficient 2 [13], in agreement with our measured value. In this regime, the acceleration plays little role as the dominant energy scales are V_R and E_σ .

IV. CONCLUSION

In conclusion, we have reported on the observation of the algebraic localization-delocalization transition with ultracold matter waves in the presence of a controlled bias force. The localized fraction of atoms only depends on a dimensionless parameter which is the ratio of the force to the disorder strength. The initial velocity only plays a role through a rescaling of the disorder strength due the correlation of the disordered potential and the localization-delocalization transition appears as an energy-independent phenomenon. Algebraic localization is observed. The observed saturation of the algebraic decay exponents at large disorder is interpreted as a consequence of a correlated and strong disorder.

Whereas adding a bias force is a natural tool to study transport in both condensed-matter and ultracold atomic disorder systems, our results show that it can have important consequences. A straightforward extension of our work can be the study of 1D *interacting* bosons in the presence of disorder, when modifying the scattering length. For example, a finite-temperature localization-delocalization phase transition has been predicted due to many-body localization effects [36]. The study of the phase diagram of 1D strongly interacting disordered Bose systems is also of interest [6,37]. Other extensions of our work could be the study of fermionic mixtures, with possibly spin-dependent forces in connection to spintronics or the response of the system to an alternating bias force

in connection with the ac conductivity in condensed-matter [38,39].

ACKNOWLEDGMENTS

We thank L. Sanchez-Palencia and A. Aspect for useful discussions. This research has been supported by CNRS, Ministère de l'Enseignement Supérieur et de la Recherche, Labex PALM, ERC Senior Grant Quantatop, Region Ile-de-France, in the framework of DIM Nano-K (IFRAF) and DIM Sirteq, EU-H2020 research and innovation program (Grant No. 641122-QUIC), Paris-Saclay, in the framework of IQUPS, Simons foundation (Award No. 563916: localization of waves).

-
- [1] C.-C. Chien, S. Peotta, and M. Di Ventra, *Nat. Phys.* **11**, 998 (2015).
- [2] M. Ben Dahan, E. Peik, J. Reichel, Y. Castin, and C. Salomon, *Phys. Rev. Lett.* **76**, 4508 (1996).
- [3] E. Haller, R. Hart, M. J. Mark, J. G. Danzl, L. Reichsöllner, M. Gustavsson, M. Dalmonte, G. Pupillo, and H.-C. Nägerl, *Nature (London)* **466**, 597 (2010).
- [4] G. Boéris, L. Gori, M. D. Hoogerland, A. Kumar, E. Lucioni, L. Tanzi, M. Inguscio, T. Giamarchi, C. D'Errico, G. Carleo, G. Modugno, and L. Sanchez-Palencia, *Phys. Rev. A* **93**, 011601(R) (2016).
- [5] L. Tanzi, E. Lucioni, S. Chaudhuri, L. Gori, A. Kumar, C. D'Errico, M. Inguscio, and G. Modugno, *Phys. Rev. Lett.* **111**, 115301 (2013).
- [6] C. D'Errico, E. Lucioni, L. Tanzi, L. Gori, G. Roux, I. P. McCulloch, T. Giamarchi, M. Inguscio, and G. Modugno, *Phys. Rev. Lett.* **113**, 095301 (2014).
- [7] S. Krinner, D. Stadler, J. Meineke, J.-P. Brantut, and T. Esslinger, *Phys. Rev. Lett.* **110**, 100601 (2013).
- [8] S. Krinner, D. Stadler, D. Husmann, J.-P. Brantut, and T. Esslinger, *Nature (London)* **517**, 64 (2015).
- [9] P. Anderson, *Phys. Rev.* **109**, 1492 (1958).
- [10] L. Sanchez-Palencia, D. Clément, P. Lugan, P. Bouyer, G. V. Shlyapnikov, and A. Aspect, *Phys. Rev. Lett.* **98**, 210401 (2007).
- [11] A. Lagendijk, B. van Tiggelen, and D. Wiersma, *Phys. Today* **62**(8), 24 (2009).
- [12] C. Gomez-Navarro, P. J. De Pablo, J. Gomez-Herrero, B. Biel, F. J. Garcia-Vidal, A. Rubio, and F. Flores, *Nat. Mater.* **4**, 534 (2005).
- [13] J. Billy, V. Josse, Z. Zuo, A. Bernard, B. Hambrecht, P. Lugan, D. Clément, L. Sanchez-Palencia, P. Bouyer, and A. Aspect, *Nature (London)* **453**, 891 (2008).
- [14] J. Chabé, G. Lemarié, B. Grémaud, D. Delande, P. Szriftgiser, and J.-C. Garreau, *Phys. Rev. Lett.* **101**, 255702 (2008).
- [15] G. Roati, C. D'Errico, L. Fallani, M. Fattori, C. Fort, M. Zaccanti, G. Modugno, M. Modugno, and M. Inguscio, *Nature (London)* **453**, 895 (2008).
- [16] E. Abrahams, P. W. Anderson, D. C. Licciardello, and T. V. Ramakrishnan, *Phys. Rev. Lett.* **42**, 673 (1979).
- [17] M. Lopez, J.-F. Clément, P. Szriftgiser, J. C. Garreau, and D. Delande, *Phys. Rev. Lett.* **108**, 095701 (2012).
- [18] F. Jendrzejewski, A. Bernard, K. Müller, P. Cheinet, V. Josse, M. Piraud, L. Pezze, L. Sanchez-Palencia, A. Aspect, and P. Bouyer, *Nat. Phys.* **8**, 392 (2012).
- [19] S. S. Kondov, W. R. McGehee, J. J. Zirbel, and B. DeMarco, *Science* **334**, 66 (2011).
- [20] G. Semeghini, M. Landini, P. Castilho, S. Roy, G. Spagnolli, A. Trenkwalder, M. Fattori, M. Inguscio, and G. Modugno, *Nat. Phys.* **11**, 554 (2015).
- [21] C. Crosnier de Bellaistre, A. Aspect, A. Georges, and L. Sanchez-Palencia, *Phys. Rev. B* **95**, 140201(R) (2017).
- [22] C. Crosnier de Bellaistre, C. Trefzger, A. Aspect, A. Georges, and L. Sanchez-Palencia, *Phys. Rev. A* **97**, 013613 (2018).
- [23] M. Hasan, M. F. Huq, and Z. H. Mahmood, *SpringerPlus* **2**, 151 (2013).
- [24] D. Clément, A. F. Varón, J. A. Retter, L. Sanchez-Palencia, A. Aspect, and P. Bouyer, *New J. Phys.* **8**, 165 (2006).
- [25] P. Lugan, A. Aspect, L. Sanchez-Palencia, D. Delande, B. Grémaud, C. A. Müller, and C. Miniatura, *Phys. Rev. A* **80**, 023605 (2009).
- [26] G. Salomon, L. Fouché, S. Lepoutre, A. Aspect, and T. Bourdel, *Phys. Rev. A* **90**, 033405 (2014).
- [27] S. Lepoutre, L. Fouché, A. Boissé, G. Berthet, G. Salomon, A. Aspect, and T. Bourdel, *Phys. Rev. A* **94**, 053626 (2016).
- [28] A. Boissé, G. Berthet, L. Fouché, G. Salomon, A. Aspect, S. Lepoutre, and T. Bourdel, *Europhys. Lett.* **117**, 10007 (2017).
- [29] M. Landini, S. Roy, G. Roati, A. Simoni, M. Inguscio, G. Modugno, and M. Fattori, *Phys. Rev. A* **86**, 033421 (2012).
- [30] C. D'Errico, M. Zaccanti, M. Fattori, G. Roati, M. Inguscio, G. Modugno, and A. Simoni, *New J. Phys.* **9**, 223 (2007).
- [31] Because of its normal incidence to the science chamber and its large coherence length, the 1064-nm laser beam produces a sub-nano-Kelvin residual periodic lattice on the atoms that can lead to Bloch oscillations [2]. We thus limit the propagation time of our experiment so that the atoms never reach the necessary velocity of 9.6 mm s^{-1} corresponding to half of the lattice wave vector.
- [32] More precisely, for reasonable integration windows extending by 200 to 500 μm along x , we still observe a sharply increasing localized fraction from 0 to 1 as a function of the disorder strength. An offset of the disorder strength corresponding to the localization transition (of the order of 10% per 100 μm)

- is observed but remains below our uncertainty (≈ 0.3) in the determination of the critical value of α .
- [33] The algebraic scaling is expected for distances $\ell \gg \ell_0$, with $\ell_0 = E/F$ and $E = mv^2/2$ the initial energy of the atoms [22]. When $v = 0$, the approximations in [22] are not valid but a sensible ℓ_0 can be estimated taking $E = V^*$. In all cases, ℓ_0 amounts to a few tens of microns in agreement with our observations.
- [34] T. Prat, N. Cherroret, and D. Delande, *Phys. Rev. A* **94**, 022114 (2016).
- [35] V. V. Volchkov, M. Pasek, V. Denechaud, M. Mukhtar, A. Aspect, D. Delande, and V. Josse, *Phys. Rev. Lett.* **120**, 060404 (2018).
- [36] I. L. Aleiner, B. L. Altshuler, and G. V. Shlyapnikov, *Nat. Phys.* **6**, 900 (2010).
- [37] T. Giamarchi and H. J. Schulz, *Phys. Rev. B* **37**, 325 (1988).
- [38] P. A. Lee and T. V. Ramakrishnan, *Rev. Mod. Phys.* **57**, 287 (1985).
- [39] R. Anderson, F. Wang, P. Xu, V. Venu, S. Trotzky, F. Chevy, and J. H. Thywissen, *Phys. Rev. Lett.* **122**, 153602 (2019).